Inorg. Chem. **2008**, *47*, 2472−2476

Crystal Growth, Structure, and Physical Properties of $SmCu_4Ga_8$

Jung Young Cho,[†] Cigdem Capan,[‡] D. P. Young,[‡] and Julia Y. Chan*[,†]

Department of Chemistry and Department of Physics and Astronomy, Louisiana State University, Baton Rouge, Louisiana 70803

Received August 31, 2007

Single crystals of $SmCu_4Ga_8$ have been grown using Ga flux and characterized by single-crystal X-ray diffraction. $SmCu_4Ga_8$, isostructural to $SmZn_{11}$, crystallizes in the hexagonal *P*6/*mmm* (No. 191) space group, with $Z = 3$ and lattice parameters $a = 8.865(2)$ Å and $c = 8.607(2)$ Å. Magnetic susceptibility data show antiferromagnetic ordering at 3.3 K. Metallic behavior is observed in the temperature range 2−300 K. A large positive magnetoresistance (MR % $= (\rho_H - \rho_0)/\rho_0 \times 100$) up to 40% is also observed near T_N. In this paper, we present the structure and physical properties of $SmCu_4Ga_8$.

Introduction

Sm-containing intermetallic compounds have attracted much attention because of the valence fluctuation between the trivalent and divalent Sm ion[1–4] and the Van Vleck paramagnetism, due to a relatively closely spaced crystal field ground state $^6H_{5/2}$ and first excited state $^6H_{7/2}$.[5,6] Because the inverse molar magnetic susceptibility is nonlinear, several Sm-based compounds such as $SmPdIn_2$,[7] $Sm_3Co_6Sn_5$,[8] SmPtIn,[9] $SmCuGa_3$,[10] and Sm_3InSe_6[11] require a modified Curie–Weiss fit. For example, $SmPdIn_2$ with the $HfNiGa_2$ structure type shows an antiferromagnetic transition and a spin reorientation at 9.0 and 5.5 K, respectively. Layered $ThCr_2Si_2$[12] structure type compounds, $SmPd_2Ga_2$[13] and $SmMn_2Ge_2$[14,15] show large magnetoresistance up to 49% and 100% at 9 T, respectively, which is unusual for most intermetallic compounds.

Ternary compounds of the Sm−Cu−Ga system adopting $NaZn_{13}$, $ThZn_{12}$, $BaCd_{11}$, $BaAl_4$, $SmZn_{11}$, and Th_2Zn_{17} have been explored by Markiv et al. at 500 °C isotherm.[16] $SmCu_{4.1}Ga_{6.9}$,[16] which is isostructural to $SmZn_{11}$,[17] shows disorder in its structure. Our ongoing exploration of the Sm−Cu−Ga ternary system using Ga flux has led us to grow single crystals of $SmCu_4Ga_8$, which is isostructural to $EuAg_4In_8$.[18] Here, we report the single crystal structure of $SmCu_4Ga_8$ and compare it to the disordered structure, $SmCu_{4.1}Ga_{6.9}$. We present the magnetism, resistivity, and magnetoresistance of $SmCu_4Ga_8$.

Experimental Section

Synthesis. Single crystals of $SmCu_4Ga_8$ were grown in excess Ga flux. Sm (3 N, Alfa Aesar) chunk, Cu powder (5 N, Alfa Aesar),

* To whom correspondence should be addressed. E-mail: jchan@lsu.edu. Telephone: (225) 578-2695. Fax: (225) 578-3458.
† Department of Chemistry.
‡ Department of Physics and Astronomy.

(1) Suga, S.; Imada, S.; Jo, T.; Taniguchi, M.; Fujimori, A.; Oh, S.-J.; Kakizaki, A.; Ishii, T.; Miyahara, T. *Phys. Rev. B: Condens. Matter* **1995**, *51*, 2061–2067.
(2) Chinchure, A. D.; Mazumdar, C.; Marathe, V. R.; Nagarajan, R.; Gupta, L. C.; Shah, S. S. *Phys. Rev. B: Condens. Matter* **1994**, *50*, 609–611.
(3) Cohen, R. L.; Eibschuetz, M.; West, K. W. *Phys. Rev. Lett.* **1970**, *24*, 383–386.
(4) Fukuhara, T.; Sakamoto, I.; Sato, H. *J. Phys.: Condens. Matter* **1991**, *3*, 8917–8929.
(5) Stewart, A. M. *Phys. Rev. B: Condens. Matter* **1993**, *47*, 11242–11246.
(6) Adachi, H.; Ino, H.; Miwa, H. *Phys. Rev. B: Condens. Matter* **1999**, *59*, 11445–11449.
(7) Zaremba, V. I.; Kaczorowski, D.; Rodewald, U. C.; Hoffmann, R.-D.; Poettgen, R. *Chem. Mater.* **2004**, *16*, 466–476.
(8) Kaczorowski, D.; Mudryk, Y.; Rogl, P.; Romaka, L.; Gorelenko, Y. *J. Phys.: Condens. Matter* **2003**, *15*, 2515–2522.
(9) Zaremba, V. I.; Galadzhun, Y. V.; Belan, B. D.; Pikul, A.; Stepien-Damm, J.; Kaczorowski, D. *J. Alloys Compd.* **2001**, *316*, 64–69.
(10) Grin, Y. N.; Hiebl, K.; Rogl, P.; Noel, H. *J. Less-Common Met.* **1990**, *162*, 371–377.
(11) Tougait, O.; Ibers, J. A. *Inorg. Chem.* **2000**, *39*, 1790–1794.
(12) Ban, Z.; Sikirica, M. *Acta Crystallogr.* **1965**, *18*, 594–599.
(13) Williams, W. M.; Macaluso, R. T.; Moldovan, M.; Young, D. P.; Chan, J. Y. *Inorg. Chem.* **2003**, *42*, 7315–7318.
(14) Van Dover, R. B.; Gyorgy, E. M.; Cava, R. J.; Krajewski, J. J.; Felder, R. J.; Peck, W. F. *Phys. Rev. B: Condens. Matter* **1993**, *47*, 6134–6137.
(15) Brabers, J. H. V. J.; Bakker, K.; Nakotte, H.; de Boer, F. R.; Lenczowski, S. K. J.; Buschow, K. H. J. *J. Alloys Compd.* **1993**, *199*, L1–L3.
(16) Markiv, V. Y.; Shevchenko, I. P.; Belyavina, N. N.; Kuzmenko, P. P. *Dopov. Akad. Nauk Ukr.* **1986**, 78–81.
(17) Mason, J. T.; Harsha, K. S.; Chiotti, P. *Acta Crystallogr., Sect. B: Struct. Sci.* **1970**, *26*, 356–361.
(18) Sysa, L. V.; Kalychak, Y. M.; Ctets, I. N.; Galadzhun, Y. V. *Kristallografiya* **1994**, *39*, 821–824.

10.1021/ic7017192 CCC: $40.75
Published on Web 03/04/2008

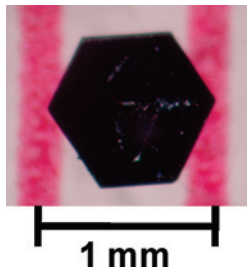

Figure 1. Single crystal of $SmCu_4Ga_8$.

Table 1. Crystallographic Parameters

Crystal Data	
formula	$SmCu_4Ga_8$
a (Å)	8.865(2)
c (Å)	8.607(2)
V (Å^3)	585.8(2)
Z	3
crystal dimension (mm^3)	0.03 × 0.03 × 0.03
cryst syst	hexagonal
space group	*P6/mmm*
θ range (°)	2.65–29.98
μ (mm^{-1})	45.027
Data Collection	
measured reflections	2187
independent reflections	393
reflections with $I > 2\sigma(I)$	369
R_{int}	0.0546
h	−12→12
k	−10→10
l	−12→12
Refinement	
$R_1[F^2 > 2\sigma(F^2)]^a$	0.0275
$wR_2(F^2)^b$	0.0606
reflections	393
parameters	30
$\Delta\rho_{max}$ (e Å^{-3})	2.520
$\Delta\rho_{min}$ (e Å^{-3})	−1.944
extinction coefficient	0.0126(5)

$^a R_1 = \sum||F_o| - |F_c||/\sum|F_o|$ $^b wR_2 = [\sum[w(F_o^2 - F_c^2)]/\sum[w(F_o^2)^2]]^{1/2}$, w = $1/[\sigma^2(F_o^2) + (0.0095P)^2 + 5.2687P]$

and Ga (6 N, Alfa Aesar) were placed into an alumina crucible in a 1:5:20 stoichiometric ratio. The crucible and its contents were then sealed in an evacuated fused silica tube and heated up to 1373 K for 7 h. After fast cooling to 773 K at a rate of 150 K/h, the tube was then slowly cooled to 673 K at a rate of 8 K/h and immediately inverted and spun with a centrifuge for the removal of excess Ga flux. Silver-colored hexagon-like crystals (Figure 1) were found and not observed to degrade in air. To ensure the complete removal of Ga on surfaces, crystals were etched using a diluted HCl (1 M) solution.

Single-Crystal X-ray Diffraction and Elemental Analysis. A 0.025 × 0.025 × 0.025 mm^3 silver-colored fragment of $SmCu_4Ga_8$ was mounted onto the goniometer of a Nonius Kappa CCD diffractometer equipped with Mo Kα radiation (λ = 0.71073 Å). Data collection was carried out up to θ = 30.0° at 298 K. Further crystallographic parameters for $SmCu_4Ga_8$ are provided in Table 1. Direct methods were used to solve the structure. SHELXL97 was used to refine the structural model of the $SmCu_4Ga_8$ compound, and data were corrected with extinction coefficients and refined with anisotropic displacement parameters. The obtained structural model was compared to the crystallographic data of $SmZn_{11}$.[17] Atomic positions and displacement parameters for $SmCu_4Ga_8$ are provided in Table 2, and selected interatomic distances are presented in Table 3. To confirm the stoichiometry of $SmCu_4Ga_8$, an inductively coupled plasma-optical emission spectroscopy (ICP-OES) experiment was performed with a Perkin-Elmer Optima Model 5300V at Galbraith Laboratories, Inc. and yielded an elemental ratio of 1:5.4:6.6 for Sm:Cu:Ga. This result suggests that it is possible for Cu to occupy some other crystallographic sites with Ga atoms. After considering of elemental analysis result, the structure of $SmCu_4Ga_8$ was carefully checked for a mixed occupancy on all of Cu and Ga sites. Cu atoms could be positioned in 6*i*, 6*k*, and 12*o* sites with statistical occupation of 2.69Cu + 3.31Ga, 2.22Cu + 3.78Ga, and 10.66Cu + 1.34Ga, respectively. This structural model gave the stoichiometry of 1:5.19:6.81 for Sm:Cu:Ga, which is close to the result of elemental analysis. However, Cu and Ga could not be distinguishable by X-ray diffraction and therefore, for simplicity, we report the stoichiometry of this compound as $SmCu_4Ga_8$ from the final structural model without mixed occupancy.

Physical Property Measurements. Magnetization data were obtained using a Quantum Design SQUID magnetometer. The temperature-dependent magnetization data were obtained under field cooled conditions from 2 to 300 K with an applied field 0.1 T. Field-dependent measurements were collected at 3 K for fields between 0 and 9 T. The electrical resistivity data were measured by the standard four-probe alternating current technique using a Quantum Design physical property measurement system.

Results and Discussion

Structure. The structure of $SmCu_4Ga_8$ is shown in Figure 2. $SmCu_4Ga_8$ is related to the disordered phase of $SmZn_{11}$[17] and isostructural to $EuAg_4In_8$.[18] $SmCu_4Ga_8$ crystallizes in the hexagonal *P6/mmm* space group (No. 191) with Sm1, Sm2, Ga1, Ga2, Ga3, Ga4, Ga5, and Cu occupying the 1*a*, 2*d*, 2*e*, 4*h*, 6*i*, 6*j*, 6*k*, and 12*o* Wyckoff sites, respectively. The crystal structure consists of two crystallographic Sm environments which are corner-sharing to each other.

Sm1 is surrounded by 12 Cu, 2 Ga1, and 6 Ga4 atoms using a cutoff of 3.42 Å as shown in Figure 3a. The Sm1 atom surrounded by six Ga4 atoms in the basal plane has a six-membered Cu ring above and below the basal plane, and the Cu rings are capped by two Ga1 atoms. The interatomic distances for Sm1−Cu, Sm1−Ga1, and Sm1−Ga4 are listed in Table 3, with interatomic distances ranging from 2.9745(15) Å to 3.3104(7) Å and agree with those in the Sm1 environment for $SmCu_{4.1}Ga_{6.9}$. The Sm2 atom also has 20 neighbors consisting of 6 Cu, 6 Ga2, 2 Ga3, and 6 Ga5 atoms (Figure 3b). Similar to the Sm1 environment, the Sm2 atom capped by two Ga3 atoms along the *c*-axis has a six-membered basal ring of Ga2 and two puckered six-membered rings composed of Cu and Ga5 above and below the basal plane. The interatomic distances of 3.0353(11) Å from to 3.416 Å for Sm2−Cu, Sm2−Ga2, Sm2−Ga3, and Sm2−Ga5 are also in good agreement with those in Sm2 polyhedra of $SmCu_{4.1}Ga_{6.9}$.[16]

A disorder was found for the $SmZn_{11}$ structure type[17] based on the observation of electron density in the difference Fourier synthesis of $SmZn_{11}$. Both the 1*b* and the 2*c* sites are positioned halfway along the *c*-axis between the 2*e* and 4*h* sites. Similar to the $SmZn_{11}$ disordered structure, $SmCu_{4.1}Ga_{6.9}$[16] has also been reported as a disordered phase. However, there was no indication of a disordered phase from our observation of the difference Fourier synthesis in our compound. During refinement, all Wyckoff positions were

Table 2. Atomic Positions and Thermal Parameters

	$SmCu_4Ga_8$						$SmZn_{11}$[a]				
Wyckoff positions	atom	*x*	*y*	*z*	occ.[b]	U_{eq} (Å^2)[c]	atom	*x*	*y*	*z*	occ.[b]
1*a*	Sm1	0	0	0	1	0.0037(2)	Sm1	0	0	0	1
2*d*	Sm2	1/3	2/3	1/2	1	0.0044(2)	Sm2	1/3	2/3	1/2	1
2*c*							Sm3	1/3	2/3	0	0.15
1*b*							Sm4	0.04	0	0	0.04
12*o*	Cu	0.16742(4)	2*x*	0.24233(7)	1	0.0077(2)	Zn1	0.1671(2)	2*x*	0.2415(3)	1
6*j*	Ga4	0.34835(11)	0	0	1	0.0097(3)	Zn2	0.3552(6)	0	0	1
6*k*	Ga5	0.29790(4)	0	1/2	1	0.0124(3)	Zn3	0.2944(5)	0	1/2	1
6*i*	Ga3	1/2	0	0.27241(12)	1	0.0123(3)	Zn4	1/2	0	0.2742(5)	1
2*e*	Ga1	0	0	0.34559(18)	1	0.0076(3)	Zn5	0	0	0.3544(8)	0.96
4*h*	Ga2	1/3	2/3	0.14734(13)	1	0.0099(3)	Zn6	1/3	2/3	0.1457(7)	0.85

[a] Obtained from ref 17. Model refined from powder X-ray diffraction data. [b] occ.: occupancy. [c] U_{eq} is defined as one-third of the trace of the orthogonalized U_{ij} tensor.

Table 3. Selected Interatomic Distances (Å)

	$SmCu_4Ga_8$
Sm1 Environment	
Sm1−Cu(×12)	3.3104(9)
Sm1−Ga1(×2)	2.9745(17)
Sm1−Ga4(×6)	3.0881(12)
Sm2 Environment	
Sm2−Cu(×6)	3.416
Sm2−Ga2(×2)	3.0353(13)
Sm2−Ga3(×6)	3.2228(8)
Sm2−Ga5(×6)	3.1239(10)
Cu/Ga Environment	
Ga1−Cu(×6)	2.7199(10)
Ga1−Ga1(×1)	2.658(3)
Ga1−Ga2(×6)	2.9564(14)
Ga2−Cu(×4)	2.5966(7)
Ga2−Ga2(×2)	2.6409(14)
Ga2−Ga5(×2)	2.6546(12)
Ga3−Cu(×3)	2.6755(9)
Ga3−Ga3(×1)	2.536(2)
Ga3−Ga5(×3)	2.7763(8)
Ga4−Cu(×4)	2.5971(7)
Ga4−Ga4(×1)	2.689(2)
Ga4−Ga5(×2)	2.7027(11)
Ga5−Cu(×4)	2.5664(7)

treated anisotropically and fully occupied. The reliable factor (R_1) and maximum residual density of 0.0275 and 2.520, respectively, confirm that this structure does not have a disorder.

$SmCu_4Ga_8$ is related to $SmCu_5$,[19,20] which belongs to the hexagonal $CaCu_5$ type,[21,22] by the following factors: $a_{SmCu_4Ga_8} \approx \sqrt{3}a_{SmCu_5}$; $c_{SmCu_4Ga_8} \approx 2c_{SmCu_5}$. When Sm atoms are replaced by pairs of Cu atoms in specific Wyckoff sites in

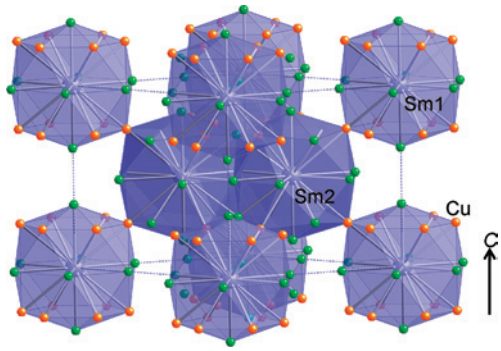

Figure 2. Crystal structure of $SmCu_4Ga_8$, where the Sm atoms are represented with blue spheres; the Cu atoms are denoted as orange spheres; and the Ga atoms are denoted with green spheres. Dashed lines are used to show the unit cell.

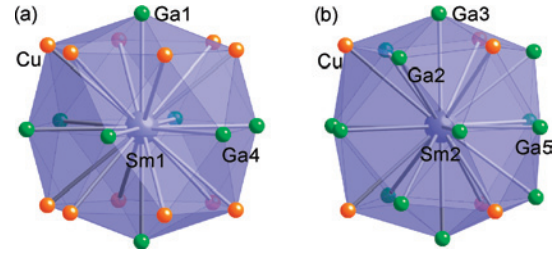

Figure 3. Local (a) Sm1 and (b) Sm2 environments.

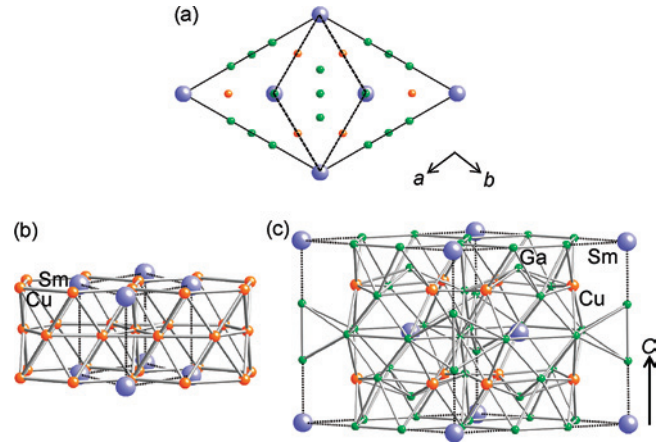

Figure 4. (a) *ab* projection and atomic arrangement of (b) $SmCu_5$ and (c) $SmCu_4Ga_8$, where the Sm, Cu, and Ga atoms are represented with blue, orange, and green spheres, respectively. The dashed and solid lines represent the unit cell of $SmCu_5$ and $SmCu_4Ga_8$, respectively.

the parental $SmCu_5$ structure type, various structure types such as $ThMn_{12}$, Th_2Fe_{17}, Th_2Ni_{17}, Th_2Zn_{17}, and U_2Zn_{17} are formed.[23] This structural relationship can be described easily through the *ab* projection and the atomic arrangement of the $SmCu_4Ga_8$ structure as shown in Figure 4a−c. The $SmCu_5$ structure has two different layers which are alternating along the *c*-axis. One is a six-membered ring layer bearing the Sm atoms in the center of hexagons. Another layer can be described as a Kagomé layer composed of Cu atoms. Within the $SmCu_4Ga_8$ structure unlike $SmCu_5$, the Kagomé layer-

(19) Svoboda, P.; Divis, M.; Bischof, J.; Smetana, Z.; Cerny, R.; Burianek, J. *Phys. Status Solidi A* **1990**, *119*, K67–K70.
(20) Svoboda, P.; Divis, M.; Gratz, E.; Cerny, R.; Dobiasova, L. *Phys. Status Solidi A* **1991**, *123*, K149–K152.
(21) Schubert, K. *Kristallstrukturen zweikomponentiger Phasen*; Springer-Verlag: Berlin, 1964.
(22) Haucke, W. *Z. Anorg. Allg. Chem.* **1940**, *244*, 17–22.
(23) Wells, A. F. *Structural Inorganic Chemistry*; 3 ed.; Oxford University Press: London, 1967.

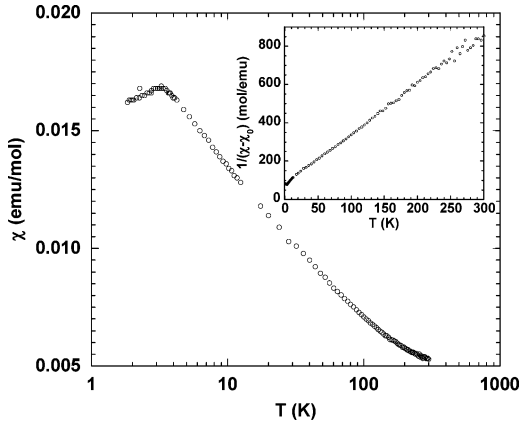

Figure 5. Magnetic susceptibility (emu/mol Sm) of $SmCu_4Ga_8$ as a function of temperature. The inset shows the inverse magnetic susceptibility from the modified Curie–Weiss law.

like hexagons are puckered by incorporation of Ga3 atoms between two different layers accompanying the systematic loss of Sm atoms.

Physical Properties. Magnetic susceptibility of $SmCu_4Ga_8$ as a function of temperature at an external field of 1 T is shown in Figure 5. The data of $SmCu_4Ga_8$ show a clear drop at 3.3 K which is indicative of an antiferromagnetic transition. From the inverse magnetic susceptibility plots of $SmCu_4Ga_8$, a curvilinear behavior in the paramagnetic region is observed (not shown), which is usually found for Sm-intermetallics, resulting from an unusual electronic structure of the Sm^{3+} ion between the $J = 5/2$ ground-state and the $J = 7/2$ excited multiplet state.[4,5,8,9,24–27] A modified Curie–Weiss equation; $\chi(T) = \chi_0 + C/(T - \theta)$ was used to obtain the magnetic moment for the Sm^{3+} ion, where χ_0 represents the temperature-independent Van Vleck term, C is the Curie constant, and θ is the Weiss temperature. The inverse modified magnetic susceptibility is fitted from 10 to 300 K and is shown in the inset of Figure 3. From this fit, the effective moment of 1.75 μ_B/Sm ion is obtained. The large negative Weiss value of −31.9 suggests strong antiferromagnetic correlations.

Figure 6 shows the isothermal magnetization data as a function of an applied field at various temperatures. The magnetization of $SmCu_4Ga_8$ increases without saturation up to 5 T which is the typical behavior of antiferromagnetic materials. As shown in Figure 6, the isothermal magnetization versus magnetic field of $SmCu_4Ga_8$ decreases with increasing temperature in the paramagnetic state. The fact that the magnetization for the 2 K isotherm is below the 3 K isotherm is a direct consequence of the antialignment of the spins below T_N in the ordered state. No metamagnetic-like anomaly was observed up to 5 T at 2K. The magnetization at 5 T is only about 0.14 μ_B, which is much smaller than the expected value of 0.71 μ_B for Sm.

The normalized temperature-dependent electrical resistance

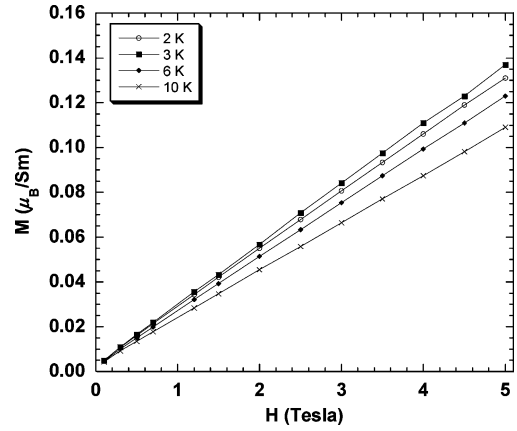

Figure 6. Magnetization of $SmCu_4Ga_8$ as a function of magnetic field at various temperatures.

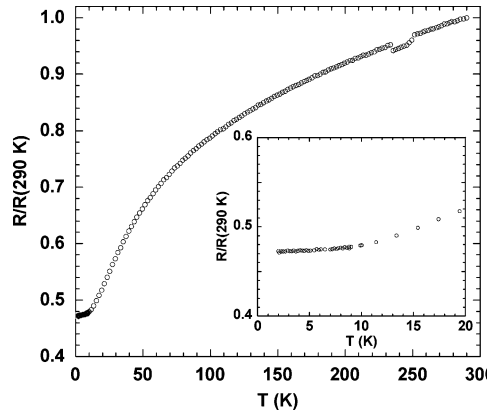

Figure 7. Normalized electrical resistance of $SmCu_4Ga_8$ as a function of temperature. The inset shows the blow-up of the normalized electrical resistance between 2 and 20 K.

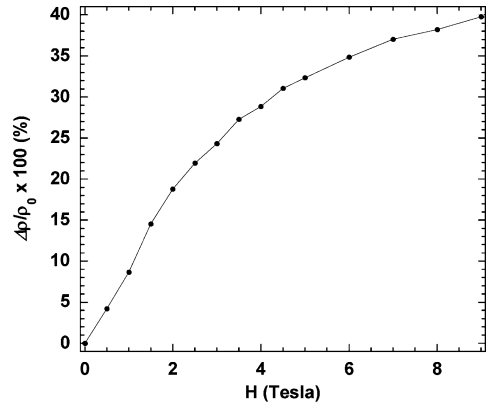

Figure 8. MR % of $SmCu_4Ga_8$ as a function of field at 3 K.

of a single crystal of $SmCu_4Ga_8$ is shown in Figure 7 and there is no indication of a kink or any anomaly at the magnetic transition as shown in the inset of Figure 7, which is quite unusual. Typically, one would expect a kink in the resistivity at the magnetic transition, indicating the reduction of spin disorder scattering. Figure 8 shows the magnetoresistance (MR = $(\rho_H - \rho_0)/\rho_0 \times 100\%$) of a single crystal of $SmCu_4Ga_8$ as a function of magnetic field at 3 K. A large positive magnetoresistance, 40% at 9 T is observed. A negative MR is typically observed because of field-suppres-

(24) Gulay, L. D.; Hiebl, K. *J. Alloys Compd.* **2003**, *351*, 35–39.
(25) Kaczorowski, D.; Gulay, L. D. *J. Alloys Compd.* **2007**, *442*, 169–171.
(26) Kaczorowski, D.; Gofryk, K.; Romaka, L.; Mudryk, Y.; Konyk, M.; Rogl, P. *Intermetallics* **2005**, *13*, 484–489.
(27) Pagliuso, P. G.; Thompson, J. D.; Hundley, M. F.; Sarrao, J. L.; Fisk, Z. *Phys. Rev. B: Condens. Matter* **2001**, *63*, 054426/1–054426/4.
(28) Usami, K. *J. Phys. Soc. Jpn.* **1978**, *45*, 466–475.

sion of spin fluctuations at the magnetic transition.[28] We, however, observe a large positive MR close to the magnetic transition. This is consistent with the absence of a kink in resistance data at T_N, suggesting that the spin-disorder scattering does not play an important role in the transport property of $SmCu_4Ga_8$. The positive sign and the saturating behavior of the MR are compatible with classical (orbital) magnetoresistance. Further work is needed to establish the origin of the positive MR. Similar behavior has been reported in $SmPd_2Ga_2$,[13] which has a large positive magnetoresistance up to 100% at 9 T and 2 K.

Acknowledgment. J.Y.C. acknowledges an NSF-CAREER award (Grant DMR0237664) and Alfred P. Sloan Fellowship for partial support of this project. D.P.Y. acknowledges an NSF-CAREER award (Grant DMR0449022).

Supporting Information Available: Additional crystallographic data in CIF format. This material is available free of charge via the Internet at http://pubs.acs.org.

IC7017192